2016 IEEE International Conference on Robotics and Automation (ICRA)
Stockholm, Sweden, May 16-21, 2016

Task Frame Estimation during Model-Based Teleoperation for Satellite Servicing

Xiao Li and Peter Kazanzides†

***Abstract*— Model-based teleoperation is suitable for systems with large communication delay because the operator interacts with a model of the task while the remote robot uses sensor-based control to replicate that interaction on the physical system. When the model geometry is accurately known, it is only necessary to register it to the remote physical system. If registration errors can be detected during the task, it is possible to update the local task frame (as in model mediated teleoperation) or the remote task frame. This paper proposes the latter approach for the case of telerobotic satellite servicing where the remote (on-orbit) robot cuts the tape that secures the patch of insulation covering the satellite access panel. This task can be modeled as sliding a tool along a planar surface (or one that is locally planar). The remote task frame is used by a hybrid position/force controller to maintain contact with the planar surface. Registration errors, however, can affect the orientation of the cutting tool and cause cutting failures. Therefore, the registration is updated during the task by using position measurements under the effect of hybrid control. The contributions of this paper are in the application of this method to teleoperation, where it must handle user-specified motions, and in the experimental verification during cutting, where compliance of the environment must be estimated and taken into account.**

I. Introduction

On-orbit satellite servicing using telerobotic technology has witnessed growing attention due to the possibility of satellite service life extension without the requirement for human presence in space. The Robotic Refueling Mission (RRM) involves tele-operation of a remote manipulator to perform tasks such as cutting through the tape that attaches the multi-layer insulation (MLI) blanket on a satellite access panel [1]. The remote robot end-effector contains a crescent-shaped cutter (Fig. 1) that is designed to separate the MLI patch over the satellite access panel by making incisions and cutting along the tape seams on three sides of the patch. This task is challenging due to a communication delay of several seconds. The refueling process begins with the spacecraft carrying the robot approaching and docking with the satellite. This process provides an initial registration of the target satellite (and thus, the MLI patch) with respect to the robot. The robot is then oriented to align the cutter axis, $\boldsymbol{z}_c$ (shown in Figure 1), with the normal of the surface, $\boldsymbol{n}_p$, underlying the patch. Hybrid position/force control [2] is used to keep the cutting tool in contact with the surface while the user teleoperates along the tangent plane to perform the cutting task [3], [4], [5]. Specifically, force control is applied along $\boldsymbol{z}_c$ while the user teleoperates in position/velocity control along $\boldsymbol{x}_c$ and $\boldsymbol{y}_c$, possibly constrained by virtual fixtures (e.g., to limit motion along $\boldsymbol{y}_c$ [6]). Typically, the orientation degrees of freedom are position controlled, with the two out-of-plane degrees of freedom (i.e., rotations about $\boldsymbol{x}_c$ and $\boldsymbol{y}_c$) fixed to maintain a desired orientation of the tool with respect to the plane normal.

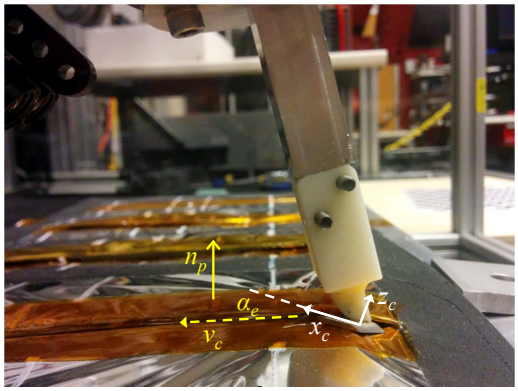

Fig. 1. Frame and vector definition. $\boldsymbol{x}_c$ is the direction of the cutter. $\boldsymbol{z}_c$ is the direction on which the normal force is measured (axis $\boldsymbol{y}_c$ can be inferred using right hand rule). $\boldsymbol{n}_p$ is the normal of the cutting surface. $\boldsymbol{v}_c$ is a vector pointing along the direction of cutting and is parallel to the cutting surface. α_e is the angle between $\boldsymbol{x}_c$ and $\boldsymbol{v}_c$

It is necessary that the cutter axis be aligned with the plane normal (within a small range of error) during the cutting task because a large misalignment will significantly reduce the task quality and is likely to cause adverse events such as the cutter digging into the access panel, potentially damaging both the robot and the satellite. This provides the incentive to estimate and correct the mis-orientation during cutting. The limited computational resources on the remote robot renders visual techniques for this real-time process impractical. Therefore, we propose a less computationally demanding online registration technique that uses only force and motion data. The use of position and/or force measurements to adjust the task frame for hybrid position/force control is well studied; some early works include [7], [8], [9]. These works focused on estimating a local task frame for a robot in contact with an unknown, or partially-known, object. A similar problem was studied by Karayiannidis and Doulgeri [10], who also assumed compliant contact with a plane and developed an adaptive controller to estimate the plane normal. This method was demonstrated in simulation, and therefore did not consider practical implementation issues.

One limitation imposed by our task is that the MLI patch is rectangular and therefore primarily straight-line motion is required to cut the tape on each side. But, a collinear

†X. Li and P. Kazanzides are with the Dept. of Computer Science, Johns Hopkins University, Baltimore, MD, USA. P. Kazanzides can be reached at pkaz@jhu.edu.

(or nearly collinear) set of points can only estimate one component of the plane normal, i.e., the orientation about y_c. In that case, the second component can only be estimated when the operator begins to cut a side of the patch that is orthogonal to the first side. The more general problem of plane estimation using data of near collinearity is studied by [11] and is referred to in the development of our method.

Relative to these prior works, one contribution of our paper is in the application to teleoperation, where the operator-specified motion can be highly variable and therefore requires some "filtering" of the motion data. A second contribution is in the experimental verification of the method on a realistic ground-based test setup.

The remaining sections are structured as follows. Section II poses an abstraction of the problem and introduces the proposed registration method. Section III introduces the experimental platform and setup followed by results and discussion in section IV. Section V concludes the paper.

II. Problem Statement and Proposed Solution

A. The Registration Problem

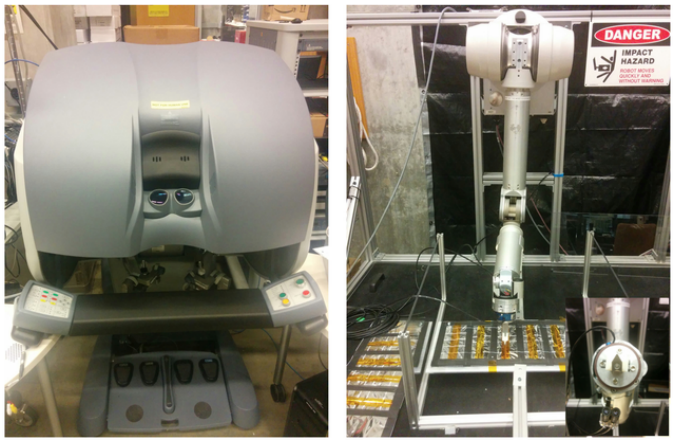

Fig. 2. Lab setup of the telerobotic cutting task. (Left) da Vinci master console. (Right) Barrett WAM as the remote manipulator performing the cutting task (small figure at bottom right shows an enlarged view of the crescent shaped cutter)

We use telerobotic cutting of the tape that secures a patch of satellite insulation as our motivating problem. This task is illustrated in Fig. 2-right, which shows the slave side of our experimental setup. The robot is a Barrett Whole Arm Manipulator (WAM), equipped with a wrist-mounted JR3 force/torque sensor. The cutter is attached to the force sensor. For this task, we assume that there is an underlying rigid planar surface (part of the satellite) and perform the cutting by pushing down (along $-\boldsymbol{z_c}$), while moving the cutter along $\boldsymbol{x_c}$ to cut the seam [5]. For cases where there is no underlying planar surface, we developed an alternate cutting strategy where we pull up on the tape seam (to create tension) while cutting [5], but we do not address that strategy in this work. Because the proposed embodiment is ground-based teleoperation of a remote on-orbit robot, the time delay is on the order of several seconds. Thus, to prevent the cutter from damaging the satellite at high contact force, we employed a hybrid position/force controller [2], with force control along the $\boldsymbol{z_c}$ direction and telerobotic position control over the robot's motion along the $\boldsymbol{x}_c$ and possibly also the $\boldsymbol{y}_c$ directions (depending on whether or not a virtual fixture is used). All orientations are under position control, and can either be fixed or adjusted telerobotically. Typically, rotations around $\boldsymbol{x}_c$ and $\boldsymbol{y}_c$ are fixed in an attempt to align the cutter (i.e., $\boldsymbol{z}_c$) with the plane normal, $\boldsymbol{n}_p$, and ensure that contact force is always as specified. We assume that the robot kinematics determine the cutter frame, $(\boldsymbol{x}_c, \boldsymbol{y}_c, \boldsymbol{z}_c)$, accurately enough with respect to the robot base frame. In the ideal case, the location of the plane is also precisely known with respect to the robot base frame. In reality, however, this transformation is only approximately known, as it is determined from measurements (e.g., from multiple camera images). Fortunately, the use of hybrid force/position control along $\boldsymbol{z}_c$ makes it unnecessary to know the position of the plane (hybrid control will force the cutter to be in contact with the cutting surface at the desired contact force), but it is necessary to know the 2DOF orientation (i.e., the plane normal, $\boldsymbol{n}_p$) so that the cutter can be aligned as described above. The goal of the proposed technique is to allow the remote robot to automatically align the cutter to the plane, during the cutting task, by estimating the 2DOF rotation between $\boldsymbol{z}_c$ and $\boldsymbol{n}_p$.

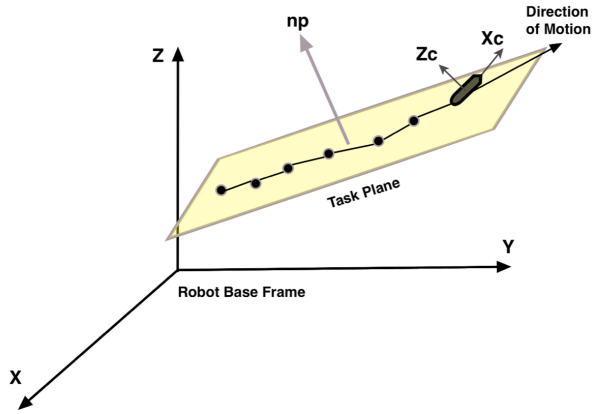

Fig. 3. Schematic of the registration problem

The registration problem can be represented by Fig. 3. The yellow plane indicates the satellite access panel that we are trying to register. The dotted line is the path that the cutter undergoes and the black dots represent positions along the path that are sampled. The goal is to use this position information along with measurements from the force sensor to perform online estimates of the plane normal $\boldsymbol{n}_p$. Since the cutter normal $\boldsymbol{z}_c$ is always known, alignment error can be calculated and corrected for. Two application specific characteristics raise the difficulty of this problem. The first issue is due to the compliance of the MLI blanket covering, as illustrated in Fig. 4. The grey solid line indicates the bottom of the access panel which is modeled as a rigid plate. The layers of dashed-lines represent the MLI, which has a thickness that the cutter can deform. If the normal

force varies during the cutting process, the sampled points will have varying offsets with respect to the underlying plate and thus will not allow an accurate estimate of the plane orientation.

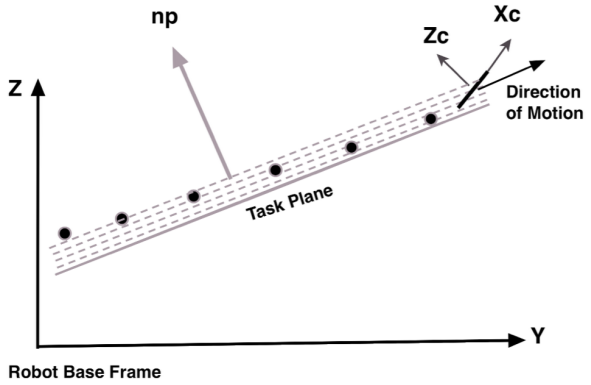

Fig. 4. Side view of task, illustrating effect of MLI compliance

The second issue arises due to the task objective, where the goal is to cut along the seams of the MLI patch. If we were to perform this task perfectly, the cutter would follow a linear path (for the first seam) and it is impossible to estimate a plane using a set of collinear points.

To summarize the registration problem, at each time step given the cutter position measurement $\boldsymbol{p}_{c_i} = [x_c, y_c, z_c]_i^T$, cutter frame orientation $R_{c_i} = [\boldsymbol{x}_c, \boldsymbol{y}_c, \boldsymbol{z}_c]_i^T$, and normal force measurement, $\boldsymbol{f}_{z_i}$, identify and correct for any misorientation that exists between the cutter and the plane normal, under conditions where the contact surface is compliant and the position measurements are likely to be highly collinear.

B. The Registration Method

Because there is no way to identify a plane through data points that are perfectly collinear, we have taken a step back to look at securing the alignment of one axis on the cutter frame. Because the robot is teleoperated, a sliding window is first adopted to filter incoming measurement data. Each measurement is defined as a position/force pair. When the most recent measurement $m_i = (p_{c_i}, f_{z_i})$ arrives, let $D = [m_1, ..., m_{i-1}]$ be the current window of data, implemented here as a first in first out (FIFO) queue. The sampling method is given by Algorithm 1.

Line 2 states that the current measurement is sampled only if it is greater than a distance l_{min} from the last sample. This is to prevent the adverse effect of clustered data on the accuracy of later registration. Note that l_{min} can be directional or not. In our analysis we have kept it a directional distance. The condition on line 4 states that whenever the number of samples in D exceeds N_{min}, discard the first sample in the window. This effectively slides the window forward. An estimation update occurs when the function returns true. Choices of the parameters l_{min} and N_{min} will be discussed in the next section.

Algorithm 1 Sliding Window Sampling

```
1:  procedure SAMPLING(p_{c_i})
2:      if |p_{c_i} − p_{c_{i−1}}| > l_min then
3:          D.Enqueue( m_i )
4:          if D.Length() > N_min then
5:              D.Dequeue( m_1 )
6:              return true
7:          else
8:              return false
9:          end if
10:     end if
11: end procedure
```

To alleviate the adverse effect of contact compliance on the accuracy of plane estimation, stiffness compensation is introduced using the simple model $\Delta z_c = k\Delta f_z$. As the cutter moves, windows of position and force data are collected; Δz_c is defined to be the difference of adjacent position data in the direction of the cutter $\boldsymbol{z}_c$ axis, and Δf_z is the difference of the corresponding measured normal forces. After a window of reasonable size of data in the form of $(\Delta z_c, \Delta f_Z)$ is obtained, the correlation of the two variables is calculated. If the correlation value exceeds a set threshold, implying that they are of acceptable linear correlation, a least square method is used to estimate the stiffness value k. Then, the z coordinate of every element in the window is shifted by:

$$z_{c_{shifted}} = \frac{f_{z_{nom}} - f_z}{k} + z_c \tag{1}$$

where $f_{z_{nom}}$ is a reference normal force, usually chosen to be the desired force of force control (in our implementation, the desired force is constant, regardless of the force applied by the operator via the master manipulator). This process effectively preserves the in-plane characteristics of the data points and minimizes their variation perpendicular to the cutting plane.

With the window of compensated data, a matrix $P_{N_{min}\times d} = [p_{c_1}, ..., p_{c_i}]^T$ is formed with columns containing the xyz coordinates of the cutter within the current window. Principal component analysis (PCA) based on singular value decomposition (SVD) is performed [11], [12] to decompose this matrix to the following form:

$$\underset{N_{min}\times d}{P} = \underset{N_{min}\times d}{U} \quad \underset{d\times d}{\Theta} \quad \underset{d\times d}{V^T} \tag{2}$$

where d is the dimension of each observation (i.e., 2 for planar position data). Components in matrix Θ are non-negative values that contain information about the amount of variation (or variance) in the principal directions. The columns of the V matrix are the corresponding principal direction vectors (in our method, matrix U is not used). If the data forms a straight line it can be expected that Θ contains only one nonzero value. Thus, we define the direction of cutting, $\boldsymbol{v}_c$, to be the direction with the largest Θ value. The angle between $\boldsymbol{x}_c$ and $\boldsymbol{v}_c$ (denoted by α_e) is monitored as

the estimated misalignment, and the correction velocity is performed by rotating the end-effector around its local axis, $\boldsymbol{y}_c$, at $vel_{corr}(deg/s)$.

Algorithm 2 Correction Velocity Calculation

procedure CORRECTION_VEL(α_e)
  if $|\alpha_e| > \alpha_{e_{upper}}$ **then**
    vel_{corr} = *sign*(α_e)$\times vel_{max}$
  else if $|\alpha_e| < \alpha_{e_{lower}}$ **then**
    $vel_{corr} = 0$
  else
    $vel_{corr} = vel_{max} \times \frac{\alpha_e}{(\alpha_{e_{upper}} - \alpha_{e_{lower}})}$
  end if
return vel_{corr}
end procedure

Algorithm 2 provides a correction velocity profile as illustrated in Figure 5. This velocity profile allows for smooth correction motions during a cutting task, as evident in the results presented in Section IV. Three parameters are to be chosen: the max correction velocity, vel_{max}, and two thresholds, $\alpha_{e_{upper}}$ and $\alpha_{e_{lower}}$. In our experiment, a positive vel_{corr} decreases α_e.

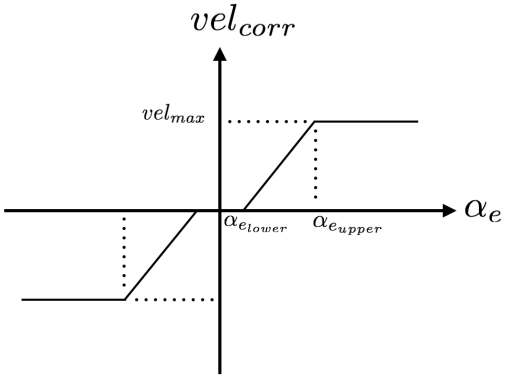

Fig. 5. Correction velocity as a function of estimated misalignment

This correction is performed until $\boldsymbol{x}_c$ is approximately parallel to $\boldsymbol{v}_c$ ($|\alpha_e| < \alpha_{e_{lower}}$). Again, with just $\boldsymbol{v}_c$ we will not be able to align the cutter and plane normal perfectly, but in our case where the cutting task is moving mostly in the direction of $\boldsymbol{x}_c$, this correction step will ensure that the cutter is oriented correctly in the direction of cutting. If the operator happens to change the direction of motion, the proposed method will be able to estimate the plane normal and perform the correction accordingly. The flowchart in Fig. 6 shows the workflow of the registration method.

III. Experimental Verification

Experimental verification of the proposed method is designed to investigate the effectiveness of stiffness estimation on compensating for material compliance (in this case, the MLI), the overall accuracy and consistency of the method's ability to estimate misalignment, and the manipulator's behavior when correcting for misalignment.

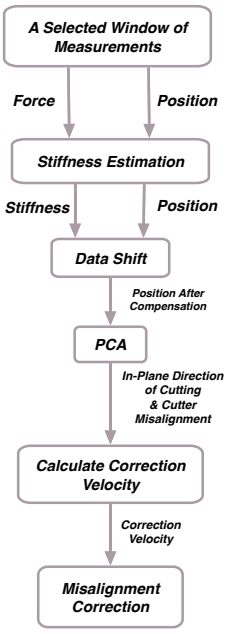

Fig. 6. Flowchart for the adaptive registration method

The robot is commanded to move forward in the $\boldsymbol{x}_c$ direction as shown in Figure 1; again, force control will ensure contact of the cutter with the cutting plane. The proposed technique will estimate the actual direction of motion, $\boldsymbol{v}_c$, and the angle this direction makes with $\boldsymbol{x}_c$, which is denoted by α_e. The first set of tests performs the cutting motion with different angles of misalignment, where the change in the angle is controlled by the robot. This test measures the relative accuracy of the estimation because while the absolute misalignment with respect to the plate is not precisely known, the difference between each misalignment angle is precisely known. The second experiment evaluates the performance of the stiffness compensation in extracting the direction of cutting, $\boldsymbol{v}_c$, under contact compliance. To obtain a more evident observation, the cutter is commanded to undergo a sinusoidal motion under force control (i.e., by varying the desired force sinusoidally) while proceeding forward with cutting. Registration results with and without stiffness compensation are compared. The final test adds misalignment correction into the process, using the correction velocity computed by Algorithm 2, and evaluates the resulting correction behavior.

Table I lists the values used for a number of parameters and thresholds in the experiment. The choice of these parameters determines the quality of data that the method uses for registration and how the correction velocity is calculated. As is described in Table I, $l_{min} = v_{max}\Delta t$, where v_{max} = 4.2 cm/s is the recorded maximum velocity from prior user tests and Δt is the sampling period (0.01 s). Choosing l_{min} this way prevents clustering of samples. N_{min} is set to 300 samples as a compromise between accuracy of estimation (higher N_{min}, as in Fig. 7-bottom) and responsiveness (lower N_{min}, as in Fig. 7-top).

TABLE I

PARAMETERS USED FOR PILOT STUDY

Parameter	Brief Description	Value
l_{min}	Minimum distance between two consecutive samples for both to be included in current window	4.2×10^{-4} (m)
N_{min}	Minimum number of samples in a window	300
$f_{z_{nom}}$	Nominal force value for data shift	0 (N)
$\alpha_{e_{upper}}$	Cutoff threshold for maximum correction velocity	3 (deg)
$\alpha_{e_{lower}}$	Cutoff threshold for zero correction velocity	0.5 (deg)
vel_{max}	Max possible correction velocity	0.05 (deg/s)

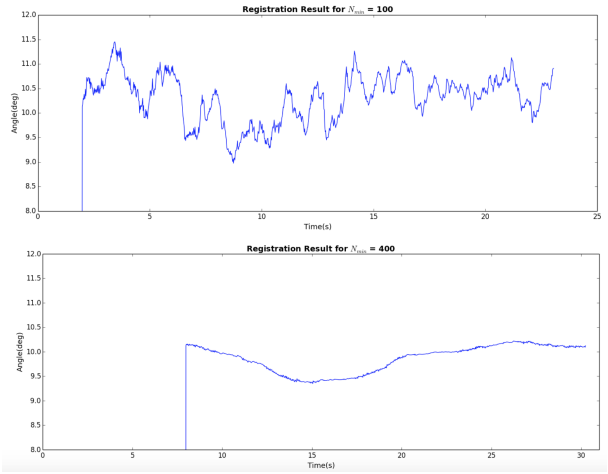

Fig. 7. Estimated misalignment angle for two N_{min} values; actual misalignment angle is approximately 10 degrees.

IV. RESULTS AND DISCUSSION

To study the registration consistency of the method over a wide range of misalignment angles, 10 tests are conducted with nominal misalignment angles ranging from 2 degrees to 20 degrees in increments of 2 degrees. The means of the resulting α_e reported by the estimator are tabulated in Table II, along with the change in α_e with respect to the preceeding test, which ideally should equal 2 degrees. The results show good relative accuracy of the method, with the difference between consecutive estimated misalignment angles generally within 0.15 degrees of the correct value and one outlier at 0.31 degrees.

The second experiment illustrates the issue of contact surface compliance (as described in Section II A) and the performance of the stiffness compensation step introduced in Section II B. Our teleoperation method specifies a constant desired normal force during cutting, regardless of the force applied by the operator in the simulated environment on the master, and therefore the effect of surface compliance is less pronounced. In fact, if the force controller worked perfectly (i.e., actual normal force equal to desired normal force) and if the MLI compliance was constant through the task, it would not be necessary to estimate compliance. In reality, however, the actual normal force varies during the cutting procedure and the MLI compliance can vary, especially in places where there are overlapping sections.

TABLE II

REGISTRATION RESULTS FOR INCREMENTAL MISALIGNMENT TEST

Nomimal angle (degrees)	Mean α_e (degrees)	Change in α_e (degrees)
2.0	1.67	-
4.0	3.98	2.31
6.0	5.88	1.90
8.0	7.87	1.99
10.0	9.86	1.99
12.0	11.93	2.07
14.0	13.79	1.86
16.0	15.92	2.13
18.0	17.80	1.88
20.0	19.67	1.87

For this experiment, the cutter was commanded to move in a sinusoidal motion along the MLI surface (i.e., by specifying a sinuoidal desired normal force), which exaggerates the effect of compliance. This is shown in Figure 8-top, where the trajectory formed by the blue dots is recorded directly from the cutter's measured position. The red dots show the trajectory after stiffness compensation. While both trajectories exhibit sinusoidal oscillation, it is significantly reduced by the stiffness compensation. Not surprisingly, Figure 8-bottom shows that the estimated misalignment computed from the uncompensated trajectory has much larger oscillations than the one computed from the compensated trajectory. Specifically, the standard deviation of the estimated misalignment angle is 1.94 degrees without stiffness compensation and 0.74 degrees with stiffness compensation. Figure 9 shows the estimated stiffness, which has a mean of 12,357.8 N/m and a standard deviation of 2,739.9 N/m. Note, however, that some of the variation may be due to actual stiffness changes in our MLI-covered test plate.

It is also important to note that while a large variation in the normal force is the worst-case scenario in estimating the direction of cutting when the effect of compliance is not compensated, it is the best-case scenario for accurate estimation of the compliance and to perform compensation.

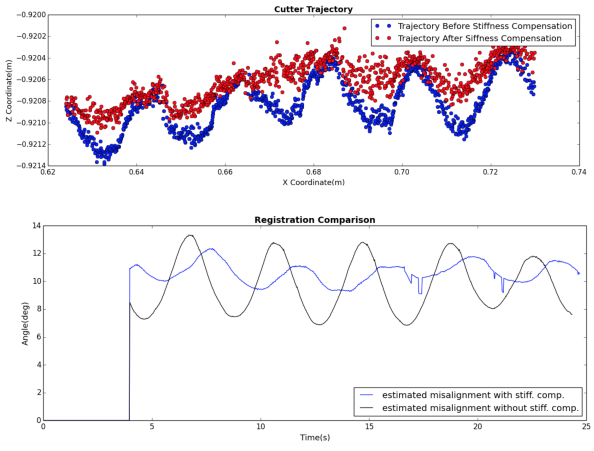

Fig. 8. Registration Results Under Sinusoidal Motion. (Top) Cutter trajectory before and after stiffness compensation. (Bottom) Estimated misalignment before and after stiffness compensation (nominal misalignment was 10 degrees)

Conversely, a minimal variation in normal force represents the worst-case scenario for estimating the compliance (in fact, our method checks for this case and does not attempt to adopt stiffness compensation for data collected in that time interval), but is the best-case scenario for estimation of the cutting direction $\boldsymbol{v}_c$. Thus the stiffness compensation step is able to compensate for compliance when $f_{z_{nom}} - f_z$ is large, and does not interfere with misalignment estimation when $f_{z_{nom}} - f_z$ is small.

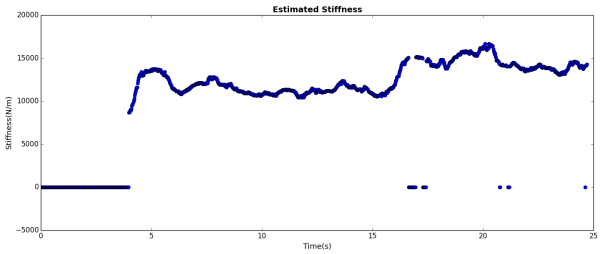

Fig. 9. Estimated stiffness. The zero stiffness values that appear after 4 seconds (which is the time for initial data collection) indicate regions where the collected data $(\Delta z_c, \Delta f_z)$ are not linearly correlated (from the correlation test described in Section II B) and stiffness estimation is not performed

In the last experiment, correction motion is incorporated into the registration process and the result is provided in Figure 10. The method for computing the angular correction velocity is provided by Algorithm 2. The cutter starts the cutting motion with a misalignment of approximately 14 degrees. The method collects initial data for about 4 seconds before starting the correction step. The result shows that the proposed method is able to effectively and smoothly reduce the misalignment and maintain the absolute value of the misalignment to within 0.5 degrees. A video showing the master and slave side view of the cutting/correction process is included.

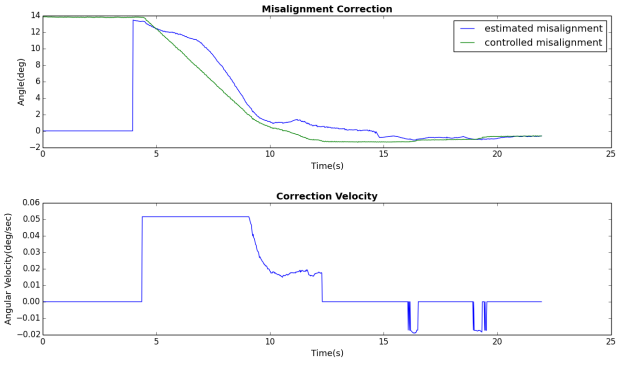

Fig. 10. Plane Registration With Correction

V. Conclusions

This paper presented a method to estimate task frame misalignment when the task is to move a tool along a plane and when force control is used to maintain contact with the plane. The registration process is intended to be applied to the adaptive alignment of the cutter tool with the target cutting surface in a telerobotic satellite servicing mission. The target surface is compliant because it is covered by a patch of MLI blanket. The task requires the cutter to move along linear path segments, which makes plane estimation difficult. The proposed method utilizes principal component analysis (PCA) in the form of singular value decomposition (SVD) to extract the direction of cutting from the measured position of the cutter. We can then estimate the angle of misalignment using this estimated cutting direction together with our knowledge of the local task frame from known robot kinematics. A sampling filter is used to ensure sufficient spatial distribution of the data. The issue of contact surface compliance is addressed by locally estimating the contact stiffness and shifting the trajectory data in the direction of force control to minimize variation with respect to the cutting plane. The method is verified experimentally and results show that accurate and consistent online estimations of the cutter misalignment can be obtained, and that the proposed algorithm computes a correction velocity that smoothly reduces the misalignment to within a specified range.

Acknowledgment

This work was supported by NASA NNG10CR16C, NNG14CR58C and NSF NRI 1208540.

References

[1] B. Roberts and J. Pellegrino, "Robotic servicing technology development," in *Proc. AIAA SPACE 2013 Conf. & Expo.*, 2013, pp. 1–10.
[2] M. H. Raibert and J. J. Craig, "Hybrid position/force control of manipulators," *ASME J. of Dynamic Systems, Measurement, and Control*, vol. 103, no. 2, pp. 126–133, Jun 1981.
[3] T. Xia, S. Léonard, A. Deguet, L. Whitcomb, and P. Kazanzides, "Augmented reality environment with virtual fixtures for robotic telemanipulation in space," in *IEEE/RSJ Intl. Conf. on Intelligent Robots and Systems (IROS)*, Oct 2012, pp. 5059–5064.
[4] T. Xia, S. Léonard, I. Kandaswamy, A. Blank, L. Whitcomb, and P. Kazanzides, "Model-based telerobotic control with virtual fixtures for satellite servicing tasks," in *IEEE Intl. Conf. on Robotics and Automation (ICRA)*, May 2013, pp. 1479–1484.
[5] I. Kandaswamy, T. Xia, and P. Kazanzides, "Strategies and models for cutting satellite insulation in telerobotic servicing missions," in *IEEE Haptics Symp.*, Feb 2014, pp. 467–472.
[6] S. Vozar, Z. Chen, P. Kazanzides, and L. L. Whitcomb, "Preliminary study of virtual nonholonomic constraints for time-delayed teleoperation," in *IEEE/RSJ Intl. Conf. on Intelligent Robots and Systems (IROS)*, Hamburg, Germany, Oct 2015.
[7] J. Merlet, "C-surface applied to the design of an hybrid force-position robot controller," in *IEEE Intl. Conf. on Robotics and Automation (ICRA)*, 1987, pp. 1055–1059.
[8] P. Kazanzides, N. S. Bradley, and W. Wolovich, "Dual-drive force/velocity control: implementation and experimental results," in *IEEE Intl. Conf. on Robotics and Automation (ICRA)*, 1989, pp. 92–97.
[9] T. Yoshikawa and A. Sudou, "Dynamic hybrid position/force control of robot manipulators-on-line estimation of unknown constraint," *IEEE Trans. on Robotics and Automation*, vol. 9, no. 2, pp. 220–226, 1993.
[10] Y. Karayiannidis and Z. Doulgeri, "An adaptive law for slope identification and force position regulation using motion variables," in *IEEE Intl. Conf. on Robotics and Automation (ICRA)*, 2006, pp. 3538–3543.
[11] J. Mandel, "Use of the singular value decomposition in regression analysis," *The American Statistician*, vol. 36, no. 1, pp. 15–24, 1982.
[12] J. Shlens, "A tutorial on principle component analysis," UCSD, Tech. Rep., 2003.